The reticulocyte restriction: invasion ligand RBP1a of *Plasmodium vivax* targets human TfR1, prohibitin-2, and basigin

Jessica Molina-Franky[1-4], Daniel Röth[1], Monica Ararat-Sarria[3,5], Manuel Alfonso Patarroyo[3,6*], Markus Kalkum[1*]

[1]Department of Immunology and Theranostics, Arthur Riggs Diabetes and Metabolism Research Institute, Beckman Research Institute of the City of Hope, Duarte, California, United States of America

[2]Global Scholars Program, Beckman Research Institute of the City of Hope, Duarte, California, United States of America

[3]Grupo de Investigación Básica en Biología Molecular e Inmunología (GIBBMI), Fundación Instituto de Inmunología de Colombia (FIDIC), Bogotá, Colombia

[4]PhD Program in Biotechnology, Universidad Nacional de Colombia, Bogotá, Colombia

[5]Health Sciences Faculty, Universidad de Ciencias Aplicadas y Ambientales (U.D.C.A), Bogotá, Colombia

[6]Microbiology Department, Faculty of Medicine, Universidad Nacional de Colombia, Bogotá, Colombia

[*] Corresponding authors:

E-mail: mkalkum@coh.org (MK)

E-mail: mapatarr.fidic@gmail.com (MAP)

Abstract

Plasmodium vivax is the most widespread malaria species with predominance in Latin America and Southeast Asia. Devising effective controls against *P. vivax* infections presents unique challenges due to the parasite's exclusive invasion of reticulocytes, a transient developmental stage of red blood cells. The ephemeral nature and limited availability of reticulocytes complicate efforts to establish continuous *in vitro* cultures to study the parasite's biology and receptor-ligand interactions. Here, the potential of the erythroid cell lines JK-1 and BEL-A as alternatives to reticulocytes was confirmed through successful parasite invasion, marking the first report of *P. vivax* entry to BEL-A cells. Furthermore, LC-MS was used to quantitatively compare the membrane proteomes of these cell lines with those of reticulocytes and mature erythrocytes. This analysis revealed significant similarities between the membrane proteomes of JK-1, BEL-A, and reticulocytes. In addition to the known *Plasmodium* receptors, transferrin receptor protein 1 (TfR1 or CD71), CD98hc, and basigin (BSG), potential receptor candidates involved in the parasite's invasion pathway were identified, including prohibitin-2 (PHB2), CAT-1 (SLC7A1), ATB(0) (SLC1A5), CD36, integrin beta-1 (ITGB1), and Metal transporter CNNM3. Proximity labeling using TurboID enabled the identification of specific interactions between PvRBP1a$_{158\text{-}650}$ and TfR1, BSG, and prohibitin-2 in the erythroid cell lines. Notably, this is the first report of prohibitin-2 as a receptor for *P. vivax*. These findings advance the understanding of *P. vivax* receptor-ligand interactions and underscore the potential of JK-1 and BEL-A cell lines as alternative models for the study of parasite biology.

Author Summary

Plasmodium vivax is a major cause of malaria, particularly in Latin America and Southeast Asia. Unlike other malaria parasites, it infects only immature red blood cells (reticulocytes), which are rare and short-lived, making laboratory studies challenging. No continuous *in vitro* culture system currently exists for *P. vivax*, limiting research into its invasion mechanisms. In this study, we evaluated two erythroid cell lines, JK-1 and BEL-A, as potential reticulocyte surrogates. We demonstrate that *P. vivax* can invade both cell types, including BEL-A cells, which had not previously been tested. Comparative analysis revealed key differences in surface protein expression between these cell lines and reticulocytes, compared to mature red blood cells, identifying seven potential parasite-receptor proteins. We further applied a proximity-based protein tagging approach to identify host-parasite interactions mediated by a specific *P. vivax* protein ligand, RBP1a. This technique revealed a potential role for prohibitin-2, TfR1, and basigin in mediating *P. vivax* entry into red blood cells by RBP1a binding. The role of prohibitin-2 as a Plasmodium receptor is a novel Discovery. Our results highlight JK-1 and BEL-A cells as valuable tools for *P. vivax* research and suggest new avenues for investigating host-pathogen interactions, with implications for malaria treatment and vaccine development.

Introduction

Malaria remains a major global health issue, with 263 million cases reported in 2023. *Plasmodium vivax*, one of the six human-infecting *Plasmodium* species, is noteworthy for its global distribution. In the Americas, most malaria cases are due to *P. vivax* (72.1%

in 2023) [1]. Its blood stage form, the merozoites, interact with red blood cell (RBC) receptors leading to RBC invasion [2–4]. However, *P. vivax* exclusively infects reticulocytes [5], immature, short-lived precursors of erythrocytes, posing a significant challenge to research progress. In contrast, *P. falciparum* has been extensively researched due to the availability of a well-established *in vitro* culture system for over 40 years [6]. This critical disparity highlights the urgent need to develop alternative research models for *P. vivax*.

The mechanism of *P. vivax* reticulocyte invasion remains unclear. It was previously believed that *P. vivax* exclusively targeted reticulocytes through the Duffy antigen receptor for chemokines (DARC) and Duffy binding protein (PvDBP) interaction [7], as individuals with the Fy(a-b-) mutation in West Africa were resistant to the infection. However, DARC is present on both reticulocytes and erythrocytes, and *P. vivax* infections have been documented in Duffy-negative populations [8–10]. Current evidence suggests that the reticulocyte-binding protein (RBP) family may play a role, interacting with transferrin receptor 1 (TfR1) and CD98 heavy chain (SLC3A2), which are lost during the maturation of reticulocytes to erythrocytes [2,3,11]. This implies that *P. vivax (*Pv*)*RBP family proteins may specifically target receptors unique to the reticulocyte membrane. Our previous studies on PvRBP1 of the *P. vivax* strain Belem (GenBank AAA29743.3) identified eleven high-affinity reticulocyte binding peptides (HABPs) corresponding to residues 158–653 of PvRBP1a in the *P. vivax* Salvador I strain (GenBank AAS85749.1). Among these, HABP 3742 (KLLGEEISEVSHLYV) and HABP 3459 (KEILDKMAKKVHYLK) exhibited dissociation constants (*K*d) of 131 nM and 155 nM, respectively [12]. Additionally, an extracellular portion of PvRBP1a,

residues 157-650, binds strongly (~50%) to reticulocytes and moderately (~20%) to erythrocytes [13]. The identity of PvRBP1a$_{157-650}$ binding-receptors within the reticulocyte membrane has been unclear. Therefore, this study evaluated the erythroleukemic cell line JK-1 [14] and the Bristol Erythroid Line Adult (BEL-A) [15] as surrogates for reticulocytes, examining their susceptibility to *P. vivax* invasion. A comparison of the cell lines' membrane proteomes revealed similarities with those of reticulocytes, and dissimilarities with erythrocyte membrane proteomes, thereby identifying potential *P. vivax* receptors. Furthermore, TurboID proximity labelling implied specific interactions of PvRBP1a$_{158-650}$ with prohibitin-2 (PHB2), TfR1, and basigin (BSG). These interactions were confirmed by ELISA, highlighting key molecular determinants of *P. vivax*'s reticulocyte tropism.

Results

P. vivax can invade the erythroid cell lines BEL-A and JK-1

Cultured BEL-A and JK-1 cells were successfully invaded by *P. vivax* from a validated mono-infected malaria patient's blood sample. The experiment required forgoing enrichment of the RBCs to 4.0% parasitemia (Fig 1 A-E). Parasite invasion was confirmed by immunofluorescence microscopy, detecting the intracellular presence of *P. vivax* lactate dehydrogenase (PvLDH), which all blood stages of the parasite are known to express [16]. PvLDH was detected in the positive control of infected reticulocytes, and in BEL-A and JK-1 cells, incubated with infected reticulocytes (Fig 2, FITC). The PvLDH signal was absent from non-infected control cells. Moreover, the presence of hemozoin (Hz) pigment, characteristic for hemoglobin consumption by *Plasmodia* within infected RBCs [17], was observed (Fig 2, bright field, and merge). The dark Hz pigment

was visible inside the parasite-infected nucleated erythroid cells as well as in infected reticulocytes that originated from the donor. Hz is an insoluble, crystallized digestion product of heme derived from the digestion of hemoglobin by malaria parasites, containing heme-derived β-hematin, which neutralizes the toxicity of free heme released after parasite invasion through a digestive process that involves the digestive vacuole structure [18]. On days 3 to 6 post-infection, no parasite-infected erythroid cells were observed, and cell mortality had substantially increased. Therefore, the experiment was stopped on day 6.

Fig 1. ***P. vivax* mono-infected reticulocytes.** (A) Three representative micrographs of *P. vivax*-infected enriched reticulocytes (red arrows) from a malaria patient. Scale bars are 3 µm. (B-D) Species-specific nested PCR for the small subunit 18S ribosomal RNA. Lane M, 100 bp marker; Lane *PvSx*, sample used in the infection of erythroid cells; Lanes *Pv*, *Pf*, and *Pm* belong to the positive controls for each species; lane NCh, negative control using genomic DNA from a healthy human; lane NC, negative control using water instead of genomic DNA. (B) *P. vivax* (~120 bp amplicon). (C) *P. falciparum* (~205 bp amplicon). (D) *P. malariae* (~144 bp amplicon). (E) DNA sequence alignment of the positive *PvSx* amplicon with the corresponding gene segment of the *P. vivax* Salvador-1 reference strain (GenBank No. XR_003001206.1) [19], showing 100% identity.

Fig 2. *P. vivax* invades BEL-A and JK-1 cells. The micrographs show *P. vivax*-infected reticulocytes as the positive Control (+); infected BEL-A and JK-1 cells at 24 and 48 h, and their non-infected negative Control (-); *P. vivax* lactate dehydrogenase (FITC

green); DNA (DAPI blue); hemozoin crystals (black dots marked with red arrows); BF (bright field); Scale bars are 5 µm.

Overlapping membrane proteomes reveal potential *P. vivax* invasion receptors

Because *P. vivax* was able to invade the erythroid BEL-A and JK-1 cells, their membranes must contain the same essential receptor molecules as reticulocytes that enable parasite invasion. Furthermore, the membranes of mature erythrocytes are expected to lack these receptors or to express them only at insufficient abundances. Consequently, a quantitative comparison of the membrane proteome of these cells with those of human reticulocytes and erythrocytes identified potential receptors for *P. vivax* merozoite ligands that are most likely responsible for its reticulocyte-restricted invasion.

Stringent isolation procedures were necessary to obtain membrane proteins of pure reticulocytes. The isolated reticulocytes ($CD71^+$, $CD45^-$) used in this proteomic comparison had a purity of 98.4% (S2 Fig). Expression of CD71 is diminished during maturation into fully functional erythrocytes [20]. Simultaneous determination of CD45 negativity was necessary, as $CD45^+$ leukocytes also express CD71, to ensure purity of the isolated reticulocytes.

The BEL-A and JK-1 cells used in the membrane proteomic comparisons were harvested from *in vitro* cultures and exhibited distinct nucleated erythroid maturation stages, including proerythroblasts, basophilic erythroblasts, polychromatic erythroblasts, and orthochromatic erythroblasts (S3 Fig), with slight dominance of the basophilic and polychromatic stages.

In total, 2,100 proteins were identified in BEL-A cells and 2,178 in JK-1 cells. The number of proteins was lower in reticulocytes (1,234) and in erythrocytes (1,347). After filtering this data for membrane proteins (see S1 Text & S4 Fig), 1,530 and 1,595 such proteins were obtained from BEL-A and JK-1 cell ghosts, respectively, while 846 and 974 proteins were identified for reticulocyte and erythrocyte ghosts.

Changes in membrane protein abundance were assessed by comparing erythroid cell lines and reticulocytes to mature erythrocytes. The protein abundancies of reticulocytes clustered better with those of BEL-A and JK-1 cells than with those of erythrocytes (Fig 3A). It was found that compared to erythrocytes 256 proteins were more abundant in reticulocytes, 1,179 in JK-1, and 1,554 in BEL-A. Of these, 144 identical proteins were increased in reticulocytes, JK-1, and BEL-A. However, reticulocytes and JK-1 cells share 18 proteins that are less abundant in erythrocytes, while BEL-A and reticulocytes

have 40 proteins in common, that are less abundant in erythrocytes. Only 54 membrane proteins with higher abundance than in erythrocytes were identified exclusively in reticulocytes, 237 in JK-1, and 590 in BEL-A cells (Fig 3B).

Fig 3. Plasma membrane proteomes of reticulocytes resemble those of erythroid cell lines. (A) Clustering of plasma membrane proteins in JK-1, BEL-A, reticulocytes, and erythrocytes, measured in triplicate. Log2 intensities. (B) Abundance of intersecting membrane proteins in reticulocytes, JK-1, and BEL-A cells compared to erythrocytes, represented in an UpSet plot [21]. 144 proteins share higher abundance among cell lines and reticulocytes but are reduced in erythrocytes (mauve bar). (C-E) Putative receptors (blue) and characterized receptors (orange) for *P. vivax* merozoite invasion. Gene names are displayed instead of protein names for simplicity. The x-axis represents the $\log_2$ fold change, and the y-axis shows the P-value, indicating statistical significance.

When comparing the membrane protein abundance in reticulocytes, cell lines, and erythrocytes, known *P. vivax* receptors such as TfR1 (CD71), CD98hc, ACKR1/DARC, BSG, CR1, and band 3 (SLC4A1) were identified. TfR1 and CD98hc, which are lost during reticulocyte maturation to erythrocytes, were significantly more abundant in reticulocytes and cell lines. In contrast, the other receptors showed higher levels in erythrocytes (Fig 3C-E).

In silico topological analysis of membrane proteins enriched in reticulocytes and erythroid cell lines identified several candidates — CD98lc (SLC7A5), high-affinity cationic amino acid transporter 1 (CAT-1, SLC7A1), neutral amino acid transporter B^0 (ATB(0), SLC1A5), CD36, Integrin β-1 (ITGB1), prohibitin-2 (PHB2), and the metal

transporter CNNM3 — as possessing sizable extracellular regions that are potentially accessible for interaction with *P. vivax* merozoite ligands (S1 Table & S5 Fig). The significantly higher abundance of these proteins in reticulocytes, BEL-A, and JK-1 cells compared to erythrocytes (Fig 3C-E & S1 Table) highlights them as potential candidates for *P. vivax* merozoite protein receptors, which may explain the parasite's exclusivity for reticulocyte invasion.

Receptors for PvRBP1a$_{158-650}$LTID identified via proximity labeling

To identify potential receptors of the PvRBP1a$_{158-650}$LTID protein, the TurboID proximity labeling technique was used. This technique enables the biotinylation of proteins that come into close contact with the fused protein (within 10 nm), facilitating the identification of their interactions [22,23]. Therefore, the fusion protein PvRBP1a$_{158-650}$LTID and the LTID control were obtained in soluble form, with PvRBP1a$_{158-650}$LTID having a molecular weight of ~94 kDa and LTID ~36 kDa (Fig 4A). Both proteins exhibited enzymatic activity and self-biotinylation at 1, 2, and 3 µM (Fig 4B-C).

Fig 4. Proximity labeling with PvRBP1a$_{158-650}$LTID in JK-1, BEL-A, reticulocytes, and erythrocytes. Recombinantly expressed soluble PvRBP1a$_{158-650}$LTID and LTID by (A) SDS PAGE (B, C) auto-biotinylation assay with increasing concentrations of each protein at 1, 2, and 3 µM, detected with IRDye 800 Streptavidin (green bands), LICORbio molecular weight markers (MW, red bands); (D) biotin labeling of JK-1 (orange) and BEL-A (fuchsia) cells, in presence of PvRBP1a$_{158-650}$LTID or LTID (negative control, JK-1 - black, and BEL-A - gray) at 1, 2, and 3 µM. (E-G) Flow cytometry (E) histograms of erythroid cells and human RBCs in presence of

PvRBP1a$_{158-650}$LTID (blue) or LTID (grey), both at 3 µM, demonstrating (F) significant degrees of cell surface labeling by PvRBP1a$_{158-650}$LTID in erythroid cells and reticulocytes compared to erythrocytes (**** $p \leq 0.0001$). (G) Receptors to PvRBP1a$_{158-650}$ are sensitive to cell surface treatment with trypsin and chymotrypsin but resistant to neuraminidase (labeling % as normalized to untreated cells).

PvRBP1a$_{158-650}$LTID exhibits comparable binding to reticulocytes and erythroid cell lines via a proteinaceous receptor

Proximity biotinylation mediated by TurboID facilitated binding evaluation through the biotin-streptavidin interaction. The assays showed that PvRBP1a$_{158-650}$LTID binding is concentration-dependent (Fig 4D). Since the highest percentage of biotin labeling on the cell surface was obtained at 3 µM, this concentration was selected to analyze PvRBP1a$_{158-650}$LTID binding to enriched reticulocytes (87.5% purity) (S6 Fig), erythrocytes, and cell lines. The results showed that PvRBP1a$_{158-650}$ had 80% biotinylation on the surface of reticulocytes, 4.7% on erythrocytes, and 79.85% and 83.2% on the surface of JK-1 and BEL-A cells, respectively. A statistically significant difference was found between the cell lines and reticulocytes compared to erythrocytes ($P \leq 0.0001$). However, no significant difference was observed between the cell lines and reticulocytes (Fig 4E-F). These data suggest that erythroid cell lines exhibit PvRBP1a$_{158-650}$ binding activity comparable to reticulocytes, indicating that they may express the receptor for this specific *P. vivax* ligand on their surface. Additionally, no labelling was detected with LTID, confirming the specificity of the PvRBP1a$_{158-650}$ receptor interaction.

Cell surface labelling with PvRBP1a$_{158-650}$LTID was sensitive to trypsin and chymotrypsin treatment but resistant to neuraminidase, which removes sialic acid from glycans that modify proteins in vertebrates (Fig 4G). Therefore, the cell surface receptor function for PvRBP1a$_{158-650}$ is proteinaceous and not dependent on sialic acid-terminated glycans.

Enrichment of PvRBP1a$_{158-650}$LTID biotinylated cell surface proteins, identifies TfR1 and prohibitin-2 as the likely reticulocyte-restricting receptors

PvRBP1a$_{158-650}$LTID biotinylated membrane proteins from erythroid cells were captured via streptavidin-affinity and subjected to proteomics analysis, revealing a total of 278 proteins, of which 12 were localized to the plasma membrane. However, the LTID control contained five of these proteins, leaving seven unique to enrichment after biotinylation with PvRBP1a$_{158-650}$LTID. Four of these membrane proteins do not possess extracellular regions, while TfR1, prohibitin-2, and BSG do. Such extracellular regions should be required to facilitate an interaction with *P. vivax* merozoite ligands (Fig 5A). Interaction of PvRBP1a$_{158-650}$ was successfully validated by targeted (PRM) LC-MS analysis for TfR1, BSG, and prohibitin-2 (Fig 5B). It clearly demonstrated that only PvRBP1a$_{158-650}$LTID biotinylated these three proteins, while LTID did not.

BSG is more abundant in erythrocytes than in reticulocytes and in the erythroid cell lines. In contrast, TfR1 and prohibitin-2 were significantly less abundant in erythrocytes (Fig 3C-E). In fact, TfR1 and prohibitin-2 were among the most abundant membrane proteins in reticulocytes and in the erythroid cell lines JK-1 and BEL-A. These findings

suggest that PvRBP1a$_{158-650}$ likely facilitate the recognition and invasion of reticulocytes through interaction with TfR1 and prohibitin-2.

Fig 5. Proximity biotin-labeled TfR1 (CD71), Basigin, and Prohibitin-2, are identified as *P. vivax* receptor candidates after interaction of JK-1 cells with PvRBP1a$_{158-650}$LTID and validated by targeted LC-MS. (A) Heatmap of labeled plasma membrane protein intensities in the PvRBP1a$_{158-650}$LITD (fuchsia) and LTID (yellow) control samples, analyzed in duplicate by DDA LC-MS proteomics. Intensities are represented on a Z-score scale, where each value was transformed by the number of standard deviations (SD) from the mean. Topology categorizes proteins by their cellular localization: intracellular (Inside, dark gray) and those with extracellular domains (Outside, cyan). They include Shroom3, GPR132 – probable G-protein coupled receptor 132, EEF1A1 – Elongation factor 1-alpha 1, protein S100-A8, protein S100-A6, TfR1, PHB2 – prohibitin-2, BSG, protein S100-A9, JUP – junction plakoglobin, DSC3 – Desmocollin-3, and VIM – vimentin. (B) Validated interactions of transferrin receptor 1, basigin, and prohibitin-2 with PvRBP1a$_{158-650}$LITD, but not with LITD, during the TurboID procedure, followed by PRM LC-MS. (1) (2) – duplicates. Stacked bars are the sum of the LC-MS ion chromatographic peak areas of the trypsin digested peptides (colored boxes) of each protein, indicating the contribution of each peptide to the individual protein abundance.

PvRBP1a$_{158-650}$LTID interacts with high-affinity binding to TfR1, BSG, and prohibitin-2

The titration curves fit well to a single-site binding saturation model. In contrast, the negative control LTID displayed a nonspecific binding pattern “unstable”, corroborating

the specificity of the interactions (Fig 6A). The Kd obtained from the ELISA titration indicated that PvRBP1a$_{158-650}$LTID had high affinity for TfR1 (Kd: 1.15 nM), followed by BSG (Kd: 2.16 nM) and prohibitin-2 (Kd: 2.77 nM) (Fig 6B).

Fig 6. PvRBP1a$_{158-650}$ binds to TfR1, BSG, and PHB2 at nanomolar affinities. (A) Titration ELISAs of protein-protein interactions between soluble ligand PvRBP1a$_{158-650}$LTID, control LTID, and the immobilized receptor candidates TfR1, BSG, and PHB2. OD_{450} absorbance values represent the binding of a TurboID-specific HRP-labeled antibody for the biotin-free quantification of ligand and control in triplicate, fitted by a single-site binding model; (B) average dissociation constants (kd) summarized as determined from the fitted titration curves above.

Discussion

This study demonstrates the utility of erythroid cell lines JK-1 and BEL-A as suitable surrogates for reticulocytes for studying the invasion process of the *P. vivax* malaria parasite. While these cell lines and their culture conditions did not support a continuous *P. vivax* culture *in vitro*, the formation of the Hz pigment and immuno detection of PvLDH strongly supported parasite invasion. In contrast to human reticulocytes, both erythroid cell lines are nucleated, which might permit them to initiate a cell-death program upon parasite invasion. Consistently, JK-1 cells were previously reported to support cell entry by both *P. vivax* and *P. falciparum* [24,25], while BEL-A cells have so far only been studied with *P. falciparum* [26]. This study is the first to report *P. vivax* invasion of BEL-A cells, confirming their susceptibility alongside JK-1 cells.

The quantitative membrane proteome comparison of reticulocytes and erythroid cell lines with erythrocytes revealed Prohibitin-2 (PHB2), TfR1 (CD71), the CD98 heavy

chain (4F2hc, gene SLC3A2), the CD98 light chain (LAT-1, gene SLC7A5), ATB(0) (gene SLC1A5), CAT-1 (SLC7A1), CD36, Integrin β-1 (gene ITGB1), and Metal transporter CNNM3 to be of significantly increased abundance in those cell lines and reticulocytes. Whereas they are strongly decreased (practically absent) in fully matured erythrocytes. The increased abundance of TfR1 and CD98 in reticulocytes over erythrocytes is consistent with previous studies [2,20]. However, genetic manipulation [3] or antibody blockade [2] of these proteins only partially reduced *P. vivax* invasion, suggesting the involvement of additional receptors. The heavy chain of CD98 (SLC3A2) was reported to be bound by *P. vivax* in immature red blood cells via PvRBP2a [2]. Therefore, other potential *P. vivax* receptor candidates with extracellular regions, namely Prohibitin-2, the CD98 light chain (LAT-1), ATB(0), CAT-1, CD36, Integrin β-1, and CNNM3 should be considered. These membrane proteins participate in various protein-protein interactions that facilitate the entry of microorganisms into host cells [27–39]. Interestingly, LAT-1, that together with its heavy chain 4F2hc forms the heteromeric CD98 [40,41], plays a role in hepatitis C virus entry [42], raising the question of whether *P. vivax* may also interact with LAT-1.

Proximity labeling of erythroid cells with PvRBP1a$_{158-650}$LTID was largely consistent with previous observations, in which ~50% of reticulocytes binding and ~20% of erythrocytes bound to PvRBP1a$_{157-650}$ [13]. Furthermore, 20 of reticulocytes and only 1% of erythrocytes bound to PvRBP1a$_{351-599}$ [43], while 31.5% of reticulocytes were reported to bind to PvRBP1a$_{30-778}$ [44]. Additionally, the trypsin and chymotrypsin sensitivity of these recombinant protein [13,43,44], as well as the PvRBP1a$_{157-653}$ HAPBs [12] align with our results.

PvRBP1a$_{158-650}$ was found to interact with Prohibitin-2, TfR1, and BSG. Prohibitin-2 and TfR1 are more abundant in reticulocyte membranes and cell lines compared to erythrocytes, while BSG is more abundant in erythrocytes. These findings suggest that PvRBP1a$_{158-650}$ may facilitate reticulocyte recognition and invasion through interaction with Prohibitin-2 and TfR1. Additionally, interaction with BSG may contribute to binding activity to erythrocytes, but not their restricted invasion, consistent with previous studies on PvRBP1a binding [12,13,43,44].

This study demonstrated strong binding of PvRBP1a$_{158-650}$ with the 89-760 domain of TfR1, contrasting with prior work that did not detect this interaction, possibly due to the crucial role of TfR1's 89-120 region, not included in the previous protein construct [25]. TfR1 is a known receptor for PvRBP2b [3], as well as for various New World arenaviruses [45,46]. BSG, a known receptor for *P. falciparum* RH5 [47,48], a member of the PfRH family homologous to the PvRBP proteins of *P. vivax* [49,50], also serves as a receptor for *P. vivax* TRAg38 [51]. Similarly, prohibitin-2, facilitates viral entry into host cells, including enteroviruses, coronaviruses, HIV-1, and flaviviruses such as dengue [39,52–54].

This research demonstrated the binding versatile of PvRBP1a$_{158-650}$, which interacts with three different membrane proteins. In biological systems, ligands often bind multiple receptors, as seen with *Plasmodium* interactions; PvTRAg38 binds both BSG and band 3 [51,55], and PfEMP1binds to several receptors [56–60].

This study demonstrates that the BEL-A and JK-1 cells are suitable models for studying *P. vivax* receptor-ligand interactions, providing viable alternatives to reticulocytes. The similarity in the abundance of potential receptor candidates between cell lines and

reticulocytes, and their dissimilarity with erythrocytes, validates the use of JK-1 and BEL-A cell lines as surrogate models for the study of *P. vivax* merozoite ligand-receptor interactions, and suggests the existence of other potential *P. vivax* receptors. prohibitin-2 and TfR1 may contribute to a redundant reticulocyte-restricted invasion pathway because they exhibit high binding affinities to PvRBP1a$_{158\text{-}650}$. These findings lay the foundation for the comprehensive study of all *P. vivax* invasion mechanisms and for the development of targeted therapies against malaria.

Materials and methods

Ethics statement

The study was conducted in accordance with the Declaration of Helsinki. Use of anonymized discarded blood from therapeutic phlebotomy was approved by the Institutional Review Board of City of Hope, Duarte, California, USA, as exempt category 4, under 45CFR46.104 (d). Blood samples from malaria patients were obtained under informed consent with the approval of the Bioethics central committee of the Universidad de Córdoba, Monteria, Colombia, and imported into the United States under CDC permit No.: 20210830-3188A0.

Collection, processing, and enrichment of *P. vivax* parasites from blood samples

P. vivax infected blood samples were collected from malaria patients in Tierralta—Córdoba, Colombia, into 5-mL sodium citrate tubes. After transportation to Bogotá, RBCs were enriched by centrifugation, mixed with an equal volume of Glycerolyte 57, cryopreserved, shipped to the U.S. lab, thawed using the NaCl method [61], and

resuspended in 3 mL of Iscove's Modified Dulbecco's Medium (IMDM). These RBCs were then enriched from 0.2% to 4.0% parasitemia by concentrating *P. vivax*-infected reticulocytes through a KCl-Percoll gradient [62]. Enrichment was evaluated by microscopy with Giemsa staining (Fig 1A).

Identification of the *Plasmodium* species

Genomic DNA was extracted from infected cells, and nested PCR was performed using this DNA to identify the *Plasmodium* species. Genus- and species-specific primers targeting the parasite's 18S ribosomal small subunit RNA were used as previously described [63] (see S1 Text).

P. vivax entry into BEL-A and JK-1 cells

The enriched *P. vivax* mono-infected RBC sample (~40 µL) was divided into two equal aliquots, one for co-incubation with BEL-A cells and the other with JK-1 cells. Each cell line ($1.5x10^5$ cells) was cultured in 500 µL of medium, for BEL-A in StemSpan serum-free expansion medium (SFEM, StemCell Technologies), containing 25% human serum (Type AB, Sigma-Aldrich), 50 ng/mL stem cell factor (SCF), 3 U/mL erythropoietin (EPO), 1 µM dexamethasone, 1 µg/mL doxycycline, 1 µg/mL chemically defined lipid concentrate (CDLC), and 100 µM hypoxanthine; and JK-1 in IMDM supplemented with GlutaMAX, with the same components, except for SCF, EPO, dexamethasone, and doxycycline. Both cultures were incubated at 37°C with 5% CO_2 and 5% O_2. Fresh medium and 2×10^5 erythroid cells were added every two days, and cultures were evaluated by immunofluorescence assay (IFA) every 24 hours for 6 days (see S1 Text).

Quantitative comparison of membrane proteomes by (DIA) - LC-MS/MS

Reticulocytes, erythrocytes, JK-1 and BEL-A cells were collected, cytoplasmic content was removed by osmolytic lysis, and membrane proteins of the remaining ghosts were extracted. From each sample, 23 µg of proteins were processed for proteomics using S-Trap columns (ProtiFi) according to the manufacturer instructions [64,65]. The resulting trypsin/LysC-digested peptides were analyzed by LC-MS/MS in data-independent acquisition (DIA) mode, as detailed in the S1 Text.

To enrich the plasma membrane proteins from the data set, proteins were filtered based on at least one of the following annotations from the UniProt subcellular localization database: “Cell membrane”, “Apical cell membrane”, “Basolateral cell membrane”, “Peripheral membrane protein” and “Plasma membrane”, and the Gene Ontology (GO) annotation term: “plasma membrane”. The topology of the membrane proteins abundant in reticulocytes compared to erythrocytes was evaluated using several predictors. Protein sequences were analyzed with Protter for overall visualization of proteoforms [66], TMHMM 2.0 for transmembrane region prediction [67], SignalP 6.0 for signal peptide identification [68], and PredGPI for GPI anchor site prediction [69].

$PvRBP1A_{158-650}$ proximity labeling for the identification of likely receptor candidates

Cloning, expression, purification, and activity of TurboID fusion proteins

The DNA sequence encoding PvRBP1a$_{158-650}$ (GenBank AAS85749.1) was derived from the *P. vivax* Salvador I reference strain (txid126793). This sequence was fused to an acidic linker (L), GDEVDEDEG, to improve solubility, and the TurboID protein (TID) [22], followed by a C-terminal 6xHis tag for purification, resulting in the PvRBP1a$_{158-650}$LTID fusion protein. An equivalent gene encoding L with TurboID alone (LTID) was designed as a negative control. Both gene constructs were obtained as customized synthetic genes, optimized for expression in *E. coli,* and cloned into a pET-28a(+) expression vector between its *Nco*I and *Xho*I sites. The constructs were expressed in soluble form in *E. coli* BL21 cells and purified by affinity chromatography, as detailed in the S1 Text. Protein purity and expression were verified by polyacrylamide gel electrophoresis. The biotinylation activity of both recombinant TurboID fusion proteins was confirmed by evaluating their autobiotinylation activity through incubation in the presence or absence of biotinylation reaction buffer Brxn (20 mM Tris-HCl, 500 µM biotin, 2.5 mM ATP, pH 7.5) at 37°C for 15 minutes, quenching on ice and Western blot analysis with streptavidin-IRDye 800CW conjugate (1:1,000) and an Odyssey DLx imaging system (LICORbio).

PvRBP1a$_{158-650}$LTID proximity labeling

To evaluate PvRBP1a$_{158-650}$LTID's interaction with JK-1, BEL-A, reticulocytes, and erythrocytes, proximity labeling assays were performed in duplicate, and repeated up to three times. Cells were washed twice with PBS supplemented with 2% human serum (HS 2%) and incubated with either PvRBP1a$_{158-650}$LTID or LTID (negative control) for 3 hours at room temperature with constant mild agitation at 10 rpm. Following incubation, cells were washed three times with HS 2% to remove unbound proteins, then incubated

with Brxn for 15 minutes at 37°C. The reaction was stopped by cooling on ice for 5 minutes, and the samples were washed with cold HS 2% before labeling with Alexa Fluor 488-conjugated streptavidin (10 µg/mL, Invitrogen) for 1 hour at room temperature. Biotinylation was quantified by cytometry, acquiring 100,000 events per sample on a FACSAria Fusion (BD). Data were analyzed with FlowJo v10.8.1 [70], calculating the percentage of biotinylated cells relative to total cells. LTID-treated and unlabeled cells served as negative controls.

The biochemical nature of PvRBP1a$_{158\text{-}650}$ receptors

JK-1 and BEL-A cells were treated with trypsin (1 mg/mL, Sigma-Aldrich), chymotrypsin (1 mg/mL, Sigma-Aldrich), or neuraminidase (50 mU, Roche) for 1 hour. After enzymatic treatment, proteolytic enzymes were inactivated with soy trypsin inhibitor (0.5 mg/mL, Sigma-Gibco) [71]. Proximity labeling assays were then performed as described above, using PvRBP1a$_{158\text{-}650}$LTID or LTID (3 µM).

Affinity enrichment and LC-MS identification of PvRBP1a$_{158\text{-}650}$ proximity-labeled receptor candidates

JK-1 cells were incubated with either PvRBP1a$_{158\text{-}650}$LTID or LTID (negative control), each at 3 µM for 3 hours. After incubation, cells were washed three times with HS 2%, then incubated with 100 µL of Brxn for 15 minutes at 37°C. The reaction was stopped as described above, and cells were resuspended in 500 µL of IP-MS lysis buffer (MS-compatible Magnetic IP kit, streptavidin, Pierce, Thermo Scientific), incubated on ice for 30 minutes with intermittent vortexing every 5 minutes. After centrifugation, the lysate's supernatant was collected and combined with Streptavidin magnetic beads (50 µL, Thermo Scientific), incubated for 1 hour at 21°C, and then overnight at 4°C, to enrich

biotinylated membrane proteins. The beads were washed, and biotinylated proteins were eluted sequentially with 100 µL of 50 mM biotin, 100 µL of elution buffer, and 100 µL of 5% SDS at 95°C.

The eluted proteins were reduced, alkylated, and processed for proteomics using S-Trap spin columns (ProtiFi) according to the manufacturer's instructions [64,65]. The resulting trypsin/LysC digested peptides were analyzed by LC-MS in data-dependent acquisition mode. Data analysis was performed using FragPipe v22.0 [72]. Candidate receptor proteins for PvRBP1a$_{158\text{-}650}$ were selected based on the presence of extracellular regions that are favorable for ligand interaction, evaluated using UniProt GO annotations and the TMHMM 2.0 predictor [67]. Receptor candidates in the PvRBP1a$_{158\text{-}650}$LTID sample that were detected in both duplicates and of significantly higher abundance (≥ 2 fold) compared to the negative control (LTID) were also considered. Subsequently, a parallel reaction monitoring (PRM) method was applied to validate and quantify the peptides of interest (as detailed in the S1 Text).

Binding affinities of *Pv*RBP1a$_{158\text{-}650}$ to select receptor candidates by ELISA

The recombinant extracellular protein domains of receptor candidates TfR1 (Cys^{89}-Phe^{760}, SinoBiological), BSG (Met^{1}-His^{205}, SinoBiological), and full-length PHB2 (Origene) were used to evaluate the interaction between the PvRBP1a$_{158\text{-}650}$ and its binding membrane proteins (S1 Fig). Maxisorp plates were coated in triplicates with 5 µg/mL of each protein for 2 hours at room temperature and blocked with SuperBlock Buffer (Thermo Scientific). Serial dilutions of PvRBP1a$_{158\text{-}650}$LTID and LTID were prepared in blocking solution, ranging from 48,000 pM to 187.5 pM (1:2 dilution) and

4,000 pM to 1.28 pM (1:5 dilution), and incubated for 16 hours at 4°C. Bound PvRBP1a$_{158-650}$LTID and LTID were detected with a TurboID-specific polyclonal rabbit antibody (anti-BirA mutated/TurboID, Agrisera, 1:10,000). After five washes with PBST, 100 µL of 3,3',5,5',-Tetramethylbenzidine (TMB) substrate was added, and the reaction was stopped with 50 µL of 1 M phosphoric acid. Absorbance was measured at 450 nm. Dissociation constants (Kd) were determined using GraphPad Prism v10.3.1 with non-linear regression and a one-site binding saturation model.

Acknowledgments

The authors are grateful to NHS Blood and Transplant, especially Professor Jan Frayne, for providing the BEL-A cell line. *"BEL-A cell lines were created by Professor Jan Frayne, Professor David Anstee and Dr Kongtana Trakarnsanga with funding from the Wellcome Trust (grant numbers 087430/Z/08 and 102610), NHS Blood and Transplant and Department of Health (England)"*. Furthermore, they wish to extend their gratitude to the "Grupo de Investigaciones Microbiológicas y Biomédicas de Córdoba – GIMBIC" from the Universidad de Córdoba, Colombia, for providing the *P. vivax* samples. This study was funded in parts by the Memorial Hermann Foundation in support of MK and JMF. The authors dedicate this study to *Professor Manuel Elkin Patarroyo (1946-2025), in loving memory.*

References

1. World Health Organization. World malaria report 2024: addressing inequity in the global malaria response. 2024.

2. Malleret B, El Sahili A, Tay MZ, Carissimo G, Ong ASM, Novera W, et al. *Plasmodium vivax* binds host CD98hc (SLC3A2) to enter immature red blood cells. Nat Microbiol. 2021;6: 991–999. doi:10.1038/s41564-021-00939-3

3. Gruszczyk J, Kanjee U, Chan L-J, Menant S, Malleret B, Lim NTY, et al. Transferrin receptor 1 is a reticulocyte-specific receptor for *Plasmodium vivax*. Science. 2018;359: 48–55. doi:10.1126/science.aan1078

4. Molina-Franky J, Patarroyo ME, Kalkum M, Patarroyo MA. The Cellular and Molecular Interaction Between Erythrocytes and *Plasmodium falciparum* Merozoites. Front Cell Infect Microbiol. 2022;12: 816574. doi:10.3389/fcimb.2022.816574

5. Malleret B, Li A, Zhang R, Tan KSW, Suwanarusk R, Claser C, et al. Plasmodium vivax: restricted tropism and rapid remodeling of CD71-positive reticulocytes. Blood. 2015;125: 1314–1324. doi:10.1182/blood-2014-08-596015

6. Trager W, Jensen JB. Human Malaria Parasites in Continuous Culture. Science. 1976;193: 673–675. doi:10.1126/science.781840

7. Horuk R, Chitnis CE, Darbonne WC, Colby TJ, Rybicki A, Hadley TJ, et al. A Receptor for the Malarial Parasite *Plasmodium vivax*: the Erythrocyte Chemokine Receptor. Science. 1993;261: 1182–1184. doi:10.1126/science.7689250

8. Ryan JR, Stoute JA, Amon J, Dunton RF, Mtalib R, Koros J, et al. Evidence for transmission of *Plasmodium vivax* among a duffy antigen negative population in Western Kenya. Am J Trop Med Hyg. 2006;75: 575–581.

9. Reyes C, Picón Jaimes YA, Kalkum M, Patarroyo MA. The Black Box of Cellular and Molecular Events of *Plasmodium vivax* Merozoite Invasion into Reticulocytes. IJMS. 2022;23: 14528. doi:10.3390/ijms232314528

10. Picón-Jaimes YA, Lozada-Martinez ID, Orozco-Chinome JE, Molina-Franky J, Acevedo-Lopez D, Acevedo-Lopez N, et al. Relationship between Duffy Genotype/Phenotype and Prevalence of *Plasmodium vivax* Infection: A Systematic Review. TropicalMed. 2023;8: 463. doi:10.3390/tropicalmed8100463

11. Galinski MR, Medina CC, Ingravallo P, Barnwell JW. A reticulocyte-binding protein complex of *Plasmodium vivax* merozoites. Cell. 1992;69: 1213–1226. doi:10.1016/0092-8674(92)90642-P

12. Urquiza M, Patarroyo M, Marí V, Ocampo M, Suarez J, Lopez R, et al. Identification and polymorphism of *Plasmodium vivax* RBP-1 peptides which bind specifically to reticulocytes. Peptides. 2002;23: 2265–2277. doi:10.1016/S0196-9781(02)00267-X

13. Ntumngia FB, Thomson-Luque R, Galusic S, Frato G, Frischmann S, Peabody DS, et al. Identification and Immunological Characterization of the Ligand Domain of

Plasmodium vivax Reticulocyte Binding Protein 1a. The Journal of Infectious Diseases. 2018;218: 1110–1118. doi:10.1093/infdis/jiy273

14. Okuno Y, Suzuki A, Ichiba S, Takahashi T, Nakamura K, Hitomi K, et al. Establishment of an Erythroid Cell Line (JK-1) that Spontaneously Diferentiates to Red Cells. 66: 8.

15. Trakarnsanga K, Griffiths RE, Wilson MC, Blair A, Satchwell TJ, Meinders M, et al. An immortalized adult human erythroid line facilitates sustainable and scalable generation of functional red cells. Nat Commun. 2017;8: 14750. doi:10.1038/ncomms14750

16. Cao P, Kho S, Grigg MJ, Barber BE, Piera KA, William T, et al. Characterisation of *Plasmodium vivax* lactate dehydrogenase dynamics in *Plasmodium vivax* infections. Commun Biol. 2024;7: 355. doi:10.1038/s42003-024-05956-6

17. Pandey AV, Tekwani BL. Formation of haemozoin/β-haematin under physiological conditions is not spontaneous. FEBS Letters. 1996;393: 189–192. doi:10.1016/0014-5793(96)00881-2

18. Coronado LM, Nadovich CT, Spadafora C. Malarial hemozoin: From target to tool. Biochimica et Biophysica Acta (BBA) - General Subjects. 2014;1840: 2032–2041. doi:10.1016/j.bbagen.2014.02.009

19. Carlton JM, Adams JH, Silva JC, Bidwell SL, Lorenzi H, Caler E, et al. Comparative genomics of the neglected human malaria parasite *Plasmodium vivax*. Nature. 2008;455: 757–763. doi:10.1038/nature07327

20. Malleret B, Li A, Zhang R, Tan KSW, Suwanarusk R, Claser C, et al. *Plasmodium vivax*: restricted tropism and rapid remodeling of CD71-positive reticulocytes. Blood. 2015;125: 1314–1324. doi:10.1182/blood-2014-08-596015

21. Lex A, Gehlenborg N, Strobelt H, Vuillemot R, Pfister H. UpSet: Visualization of Intersecting Sets. IEEE Trans Visual Comput Graphics. 2014;20: 1983–1992. doi:10.1109/TVCG.2014.2346248

22. Branon TC, Bosch JA, Sanchez AD, Udeshi ND, Svinkina T, Carr SA, et al. Efficient proximity labeling in living cells and organisms with TurboID. Nat Biotechnol. 2018;36: 880–887. doi:10.1038/nbt.4201

23. Cho KF, Branon TC, Udeshi ND, Myers SA, Carr SA, Ting AY. Proximity labeling in mammalian cells with TurboID and split-TurboID. Nat Protoc. 2020;15: 3971–3999. doi:10.1038/s41596-020-0399-0

24. Kanjee U, Grüring C, Chaand M, Lin K-M, Egan E, Manzo J, et al. CRISPR/Cas9 knockouts reveal genetic interaction between strain-transcendent erythrocyte determinants of *Plasmodium falciparum* invasion. Proc Natl Acad Sci U S A. 2017;114: E9356–E9365. doi:10.1073/pnas.1711310114

25. Gruszczyk J, Kanjee U, Chan L-J, Menant S, Malleret B, Lim NTY, et al. Transferrin receptor 1 is a reticulocyte-specific receptor for *Plasmodium vivax*. Science. 2018;359: 48–55. doi:10.1126/science.aan1078

26. Satchwell TJ, Wright KE, Haydn-Smith KL, Sánchez-Román Terán F, Moura PL, Hawksworth J, et al. Genetic manipulation of cell line derived reticulocytes enables dissection of host malaria invasion requirements. Nat Commun. 2019;10: 3806. doi:10.1038/s41467-019-11790-w

27. Smith JosephD, Kyes S, Craig AlisterG, Fagan T, Hudson-Taylor D, Miller LouisH, et al. Analysis of adhesive domains from the A4VAR Plasmodium falciparum erythrocyte membrane protein-1 identifies a CD36 binding domain. Molecular and Biochemical Parasitology. 1998;97: 133–148. doi:10.1016/S0166-6851(98)00145-5

28. Albritton LM, Kim JW, Tseng L, Cunningham JM. Envelope-binding domain in the cationic amino acid transporter determines the host range of ecotropic murine retroviruses. J Virol. 1993;67: 2091–2096. doi:10.1128/jvi.67.4.2091-2096.1993

29. Yoshimoto T, Yoshimoto E, Meruelo D. Identification of amino acid residues critical for infection with ecotropic murine leukemia retrovirus. J Virol. 1993;67: 1310–1314. doi:10.1128/jvi.67.3.1310-1314.1993

30. Olaya-Galán NN, Salas-Cárdenas SP, Rodriguez-Sarmiento JL, Ibáñez-Pinilla M, Monroy R, Corredor-Figueroa AP, et al. Risk factor for breast cancer development under exposure to bovine leukemia virus in Colombian women: A case-control study. Jaworski JP, editor. PLoS ONE. 2021;16: e0257492. doi:10.1371/journal.pone.0257492

31. Tailor CS, Nouri A, Zhao Y, Takeuchi Y, Kabat D. A sodium-dependent neutral-amino-acid transporter mediates infections of feline and baboon endogenous retroviruses and simian type D retroviruses. J Virol. 1999;73: 4470–4474. doi:10.1128/JVI.73.5.4470-4474.1999

32. Feire AL, Roy RM, Manley K, Compton T. The Glycoprotein B Disintegrin-Like Domain Binds Beta 1 Integrin To Mediate Cytomegalovirus Entry. J Virol. 2010;84: 10026–10037. doi:10.1128/JVI.00710-10

33. Xiao J, Palefsky JM, Herrera R, Berline J, Tugizov SM. The Epstein–Barr virus BMRF-2 protein facilitates virus attachment to oral epithelial cells. Virology. 2008;370: 430–442. doi:10.1016/j.virol.2007.09.012

34. Weigel-Kelley KA, Yoder MC, Srivastava A. α5β1 integrin as a cellular coreceptor for human parvovirus B19: requirement of functional activation of β1 integrin for viral entry. Blood. 2003;102: 3927–3933. doi:10.1182/blood-2003-05-1522

35. Graham KL, Halasz P, Tan Y, Hewish MJ, Takada Y, Mackow ER, et al. Integrin-Using Rotaviruses Bind α2β1 Integrin α2 I Domain via VP4 DGE Sequence and

Recognize αXβ2 and αVβ3 by Using VP7 during Cell Entry. J Virol. 2003;77: 9969–9978. doi:10.1128/JVI.77.18.9969-9978.2003

36. Maginnis MS, Forrest JC, Kopecky-Bromberg SA, Dickeson SK, Santoro SA, Zutter MM, et al. Beta1 integrin mediates internalization of mammalian reovirus. J Virol. 2006;80: 2760–2770. doi:10.1128/JVI.80.6.2760-2770.2006

37. Nägele V, Heesemann J, Schielke S, Jiménez-Soto LF, Kurzai O, Ackermann N. Neisseria meningitidis adhesin NadA targets beta1 integrins: functional similarity to Yersinia invasin. J Biol Chem. 2011;286: 20536–20546. doi:10.1074/jbc.M110.188326

38. Wintachai P, Wikan N, Kuadkitkan A, Jaimipuk T, Ubol S, Pulmanausahakul R, et al. Identification of prohibitin as a Chikungunya virus receptor protein. J Med Virol. 2012;84: 1757–1770. doi:10.1002/jmv.23403

39. Su W, Huang S, Zhu H, Zhang B, Wu X. Interaction between PHB2 and Enterovirus A71 VP1 Induces Autophagy and Affects EV-A71 Infection. Viruses. 2020;12: 414. doi:10.3390/v12040414

40. Lee Y, Wiriyasermkul P, Jin C, Quan L, Ohgaki R, Okuda S, et al. Cryo-EM structure of the human L-type amino acid transporter 1 in complex with glycoprotein CD98hc. Nat Struct Mol Biol. 2019;26: 510–517. doi:10.1038/s41594-019-0237-7

41. Yan R, Zhao X, Lei J, Zhou Q. Structure of the human LAT1–4F2hc heteromeric amino acid transporter complex. Nature. 2019;568: 127–130. doi:10.1038/s41586-019-1011-z

42. Nguyen NNT, Lim Y-S, Nguyen LP, Tran SC, Luong TTD, Nguyen TTT, et al. Hepatitis C Virus Modulates Solute carrier family 3 member 2 for Viral Propagation. Sci Rep. 2018;8: 15486. doi:10.1038/s41598-018-33861-6

43. Han J-H, Lee S-K, Wang B, Muh F, Nyunt MH, Na S, et al. Identification of a reticulocyte-specific binding domain of *Plasmodium vivax* reticulocyte-binding protein 1 that is homologous to the PfRh4 erythrocyte-binding domain. Sci Rep. 2016;6: 26993. doi:10.1038/srep26993

44. Gupta ED, Anand G, Singh H, Chaddha K, Bharti PK, Singh N, et al. Naturally Acquired Human Antibodies Against Reticulocyte-Binding Domains of *Plasmodium vivax* Proteins, PvRBP2c and PvRBP1a, Exhibit Binding-Inhibitory Activity. J Infect Dis. 2017;215: 1558–1568. doi:10.1093/infdis/jix170

45. Radoshitzky SR, Kuhn JH, Spiropoulou CF, Albariño CG, Nguyen DP, Salazar-Bravo J, et al. Receptor determinants of zoonotic transmission of New World hemorrhagic fever arenaviruses. Proc Natl Acad Sci USA. 2008;105: 2664–2669. doi:10.1073/pnas.0709254105

46. Radoshitzky SR, Abraham J, Spiropoulou CF, Kuhn JH, Nguyen D, Li W, et al. Transferrin receptor 1 is a cellular receptor for New World haemorrhagic fever arenaviruses. Nature. 2007;446: 92–96. doi:10.1038/nature05539

47. Crosnier C, Bustamante LY, Bartholdson SJ, Bei AK, Theron M, Uchikawa M, et al. Basigin is a receptor essential for erythrocyte invasion by *Plasmodium falciparum*. Nature. 2011;480: 534–537. doi:10.1038/nature10606

48. Chen L, Xu Y, Healer J, Thompson JK, Smith BJ, Lawrence MC, et al. Crystal structure of PfRh5, an essential *Plasmodium falciparum* ligand for invasion of human erythrocytes. eLife. 2014;3: e04187. doi:10.7554/eLife.04187

49. Rayner JC, Galinski MR, Ingravallo P, Barnwell JW. Two Plasmodium falciparum genes express merozoite proteins that are related to Plasmodium vivax and Plasmodium yoelii adhesive proteins involved in host cell selection and invasion. Proceedings of the National Academy of Sciences. 2000;97: 9648–9653. doi:10.1073/pnas.160469097

50. Triglia T, Thompson J, Caruana SR, Delorenzi M, Speed T, Cowman AF. Identification of Proteins from Plasmodium falciparum That Are Homologous to Reticulocyte Binding Proteins in Plasmodium vivax. Petri WA, editor. Infect Immun. 2001;69: 1084–1092. doi:10.1128/IAI.69.2.1084-1092.2001

51. Rathore S, Dass S, Kandari D, Kaur I, Gupta M, Sharma YD. Basigin Interacts with *Plasmodium vivax*Tryptophan-rich Antigen PvTRAg38 as a Second Erythrocyte Receptor to Promote Parasite Growth. J Biol Chem. 2017;292: 462–476. doi:10.1074/jbc.M116.744367

52. Emerson V, Holtkotte D, Pfeiffer T, Wang I-H, Schnölzer M, Kempf T, et al. Identification of the Cellular Prohibitin 1/Prohibitin 2 Heterodimer as an Interaction Partner of the C-Terminal Cytoplasmic Domain of the HIV-1 Glycoprotein. J Virol. 2010;84: 1355–1365. doi:10.1128/JVI.01641-09

53. Cornillez-Ty CT, Liao L, Yates JR, Kuhn P, Buchmeier MJ. Severe acute respiratory syndrome coronavirus nonstructural protein 2 interacts with a host protein complex involved in mitochondrial biogenesis and intracellular signaling. J Virol. 2009;83: 10314–10318. doi:10.1128/JVI.00842-09

54. Kuadkitkan A, Wikan N, Fongsaran C, Smith DR. Identification and characterization of prohibitin as a receptor protein mediating DENV-2 entry into insect cells. Virology. 2010;406: 149–161. doi:10.1016/j.virol.2010.07.015

55. Alam MS, Rathore S, Tyagi RK, Sharma YD. Host-parasite interaction: multiple sites in the *Plasmodium vivax* tryptophan-rich antigen PvTRAg38 interact with the erythrocyte receptor band 3. Griesinger C, editor. FEBS Lett. 2016;590: 232–241. doi:10.1002/1873-3468.12053

56. Yipp BG, Anand S, Schollaardt T, Patel KD, Looareesuwan S, Ho M. Synergism of multiple adhesion molecules in mediating cytoadherence of *Plasmodium falciparum*–infected erythrocytes to microvascular endothelial cells under flow. Blood. 2000;96: 2292–2298. doi:10.1182/blood.V96.6.2292

57. Vogt AM, Barragan A, Chen Q, Kironde F, Spillmann D, Wahlgren M. Heparan sulfate on endothelial cells mediates the binding of *Plasmodium falciparum*–infected erythrocytes via the DBL1α domain of PfEMP1. Blood. 2003;101: 2405–2411. doi:10.1182/blood-2002-07-2016

58. Vigan-Womas I, Guillotte M, Juillerat A, Hessel A, Raynal B, England P, et al. Structural Basis for the ABO Blood-Group Dependence of *Plasmodium falciparum* Rosetting. Rowe JA, editor. PLoS Pathog. 2012;8: e1002781. doi:10.1371/journal.ppat.1002781

59. Kessler A, Dankwa S, Bernabeu M, Harawa V, Danziger SA, Duffy F, et al. Linking EPCR-Binding PfEMP1 to Brain Swelling in Pediatric Cerebral Malaria. Cell Host & Microbe. 2017;22: 601-614.e5. doi:10.1016/j.chom.2017.09.009

60. Esser C, Bachmann A, Kuhn D, Schuldt K, Förster B, Thiel M, et al. Evidence of promiscuous endothelial binding by *Plasmodium falciparum*-infected erythrocytes. Cell Microbiol. 2014;16: 701–708. doi:10.1111/cmi.12270

61. Blomqvist, K. Thawing of glycerolyte-frozen parasites with NaCl. Methods in Malaria Research. MR4/ATCC, Manassas. Methods in Malaria Research. Methods in Malaria Research. MR4/ATCC, Manassas. 2008. p. 15.

62. Rangel GW, Clark MA, Kanjee U, Lim C, Shaw-Saliba K, Menezes MJ, et al. Enhanced ex vivo *Plasmodium vivax* Intraerythrocytic Enrichment and Maturation for Rapid and Sensitive Parasite Growth Assays. Antimicrob Agents Chemother. 2018;62: e02519-17. doi:10.1128/AAC.02519-17

63. Snounou G, Viriyakosol S, Xin Ping Zhu, Jarra W, Pinheiro L, Do Rosario VE, et al. High sensitivity of detection of human malaria parasites by the use of nested polymerase chain reaction. Molecular and Biochemical Parasitology. 1993;61: 315–320. doi:10.1016/0166-6851(93)90077-B

64. HaileMariam M, Eguez RV, Singh H, Bekele S, Ameni G, Pieper R, et al. S-Trap, an Ultrafast Sample-Preparation Approach for Shotgun Proteomics. J Proteome Res. 2018;17: 2917–2924. doi:10.1021/acs.jproteome.8b00505

65. Matulis D. Selective Precipitation of Proteins. CP Protein Science. 2016;83. doi:10.1002/0471140864.ps0405s83

66. Omasits U, Ahrens CH, Müller S, Wollscheid B. Protter: interactive protein feature visualization and integration with experimental proteomic data. Bioinformatics. 2014;30: 884–886. doi:10.1093/bioinformatics/btt607

67. Hallgren J, Tsirigos KD, Pedersen MD, Almagro Armenteros JJ, Marcatili P, Nielsen H, et al. DeepTMHMM predicts alpha and beta transmembrane proteins using deep neural networks. Bioinformatics; 2022 Apr. doi:10.1101/2022.04.08.487609

68. Teufel F, Almagro Armenteros JJ, Johansen AR, Gíslason MH, Pihl SI, Tsirigos KD, et al. SignalP 6.0 predicts all five types of signal peptides using protein language models. Nat Biotechnol. 2022;40: 1023–1025. doi:10.1038/s41587-021-01156-3

69. Pierleoni A, Martelli PL, Casadio R. PredGPI: a GPI-anchor predictor. BMC Bioinformatics. 2008;9: 392. doi:10.1186/1471-2105-9-392

70. Ashland, OR: Becton, Dickinson and Company. FlowJo™ Software (for Windows) Version 10.8.1. 2023.

71. Deans A-M, Nery S, Conway DJ, Kai O, Marsh K, Rowe JA. Invasion Pathways and Malaria Severity in Kenyan *Plasmodium falciparum* Clinical Isolates. Infect Immun. 2007;75: 3014–3020. doi:10.1128/IAI.00249-07

72. Yu F, Haynes SE, Nesvizhskii AI. IonQuant Enables Accurate and Sensitive Label-Free Quantification With FDR-Controlled Match-Between-Runs. Molecular & Cellular Proteomics. 2021;20: 100077. doi:10.1016/j.mcpro.2021.100077

Supporting information captions

S1 Text. Supporting methods.

S1 Table. *P. vivax* merozoite candidate receptors

S1 Fig. Purity Analysis of Recombinant Proteins.

Recombinant proteins BSG, TfR1, and PHB2 were separated on a 4–12% polyacrylamide gel and stained with Coomassie blue. The observed bands correspond to the expected molecular weights for each protein: BSG (35 kDa), TfR1 (~77.4 kDa), and PHB2 (~35.7 kDa), confirming their purity. The Kaleidoscope molecular weight marker (Bio-Rad) is included in the left lane as a reference.

S2 Fig. Reticulocyte enrichment.

(A, B) Reticulocyte percentage in the initial whole blood sample. (C, D) Reticulocyte percentage after Percoll density (70%-62%) enrichment. (E) Purity of reticulocytes

(CD71^{+} CD45^{-}) after sorting collection. This high-purity reticulocyte sample was not evaluated with brilliant cresyl blue due to the small total volume of sample obtained (~ 50 µL). (B, D) Blood smears stained with brilliant cresyl blue to identify reticulocytes (red arrows). Scale bars are 10 µm.

S3 Fig. Differentiation of erythroid cells.

(A-D) BEL-A cells. (E-H) JK-1 cells. (A, E) Proerythroblasts (20-25 µm) were identified by their large nucleus with fine chromatin, prominent nucleoli, and basophilic cytoplasm. These cells progressed to (B, F) Basophilic erythroblasts (16-18 µm), characterized by a slightly smaller nucleus with condensed chromatin and cytoplasm with pronounced basophilia due to increased ribosomes synthesizing Hb. Subsequently, cells differentiated into (C, G) polychromatophilic erythroblasts (12-15 µm), which exhibited a more condensed nucleus with clusters of heterochromatin. The final nucleated stage, (D, H) orthochromatic erythroblast, indicated by the red arrow in D (10-12 µm), was noted for its pyknotic nucleus and a cytoplasm rich in acidophilic Hb. At this stage, the nucleus is expelled to form reticulocytes (8-10 µm), which then mature into erythrocytes (7-8 µm) through the final step of erythroid differentiation.

S4 Fig. Gene Ontology (GO) term analysis of plasma membrane proteins.

Scatterplots showing the GO terms: cellular component, molecular function, and biological process of enriched plasma membrane proteins. The bubble color indicates the count of the GO term, which was obtained from the DAVID functional annotation charts. The size of the bubbles indicates the frequency of the GO term in the Gene Ontology Annotation (GOA) database. The axes of the plot have no intrinsic meaning. REVIGO (version 1.8.1) was used to generate these scatterplots by reducing the

dimensionality of a pairwise semantic similarity matrix of GO terms using Multidimensional Scaling (MDS). The resulting projection is not nonlinear. The guiding principle is that semantically similar GO terms should remain close together in the plot.

S5 Fig. Topology of *P. vivax* merozoite receptor candidates.

(A-J) Predicted locations of potential parasite receptors are illustrated for the signal peptide (yellow), extracellular domain (blue), intracellular domain (mauve), and membrane-embedded domain (red).

S6 Fig. Reticulocyte enrichment process.

(A) Initial percentage of reticulocytes in the whole blood sample (0.11%). (B) Percentage of reticulocytes after enrichment using a 70%-62% Percoll density gradient (10.5%). (C) Final percentage of reticulocytes ($CD45^-$ and $CD98^+$) following FACS sorting (87.5%).

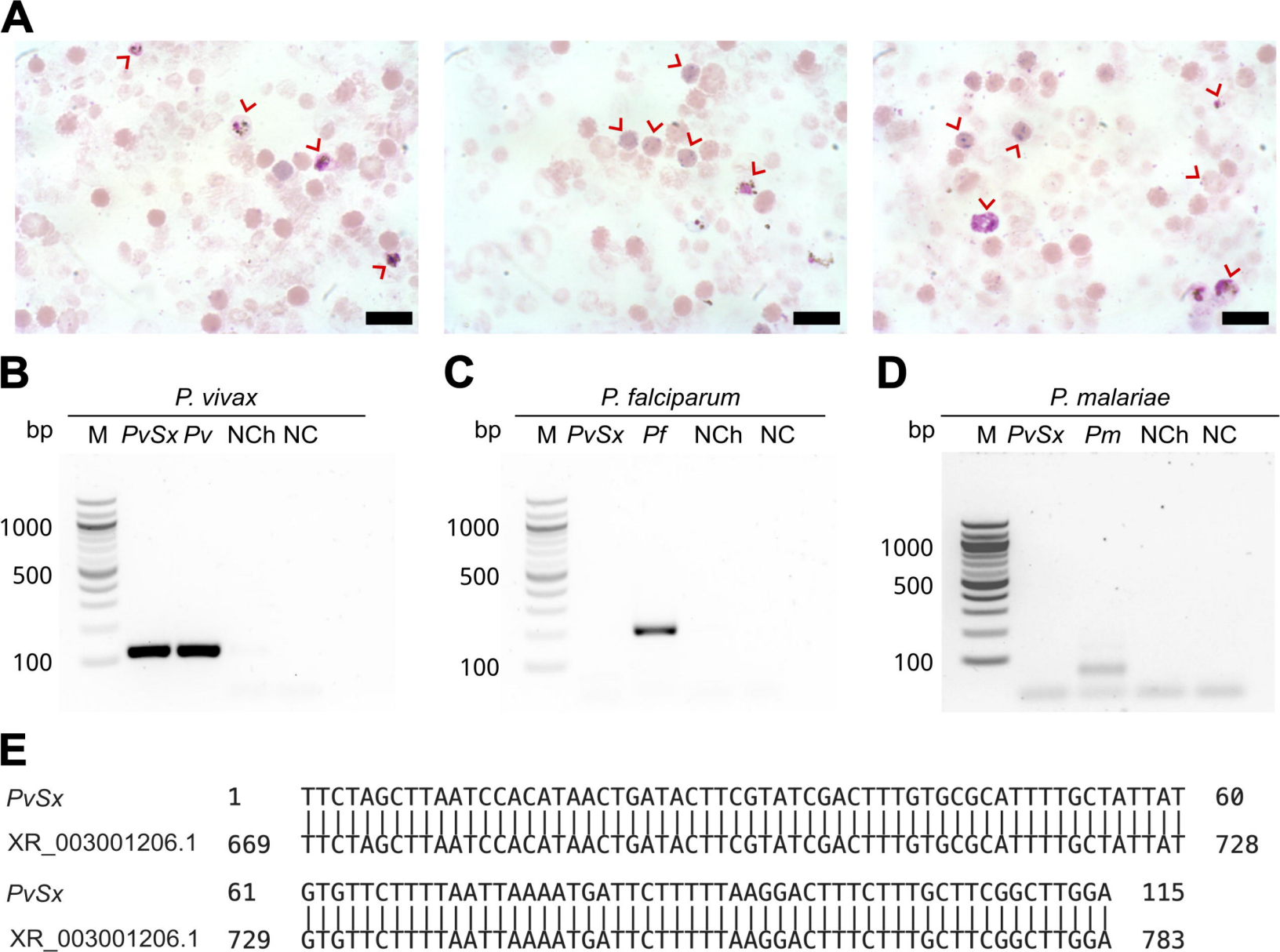
A
B
P. vivax
bp
M PvSx Pv NCh NC
1000
500
100
C
P. falciparum
bp
M PvSx Pf NCh NC
1000
500
100
D
P. malariae
bp
M PvSx Pm NCh NC
1000
500
100
E
PvSx 1 TTCTAGCTTAATCCACATAACTGATACTTCGTATCGACTTTGTGCGCATTTTGCTATTAT 60
XR_003001206.1 669 TTCTAGCTTAATCCACATAACTGATACTTCGTATCGACTTTGTGCGCATTTTGCTATTAT 728
PvSx 61 GTGTTCTTTTAATTAAAATGATTCTTTTTAAGGACTTTCTTTGCTTCGGCTTGGA 115
XR_003001206.1 729 GTGTTCTTTTAATTAAAATGATTCTTTTTAAGGACTTTCTTTGCTTCGGCTTGGA 783

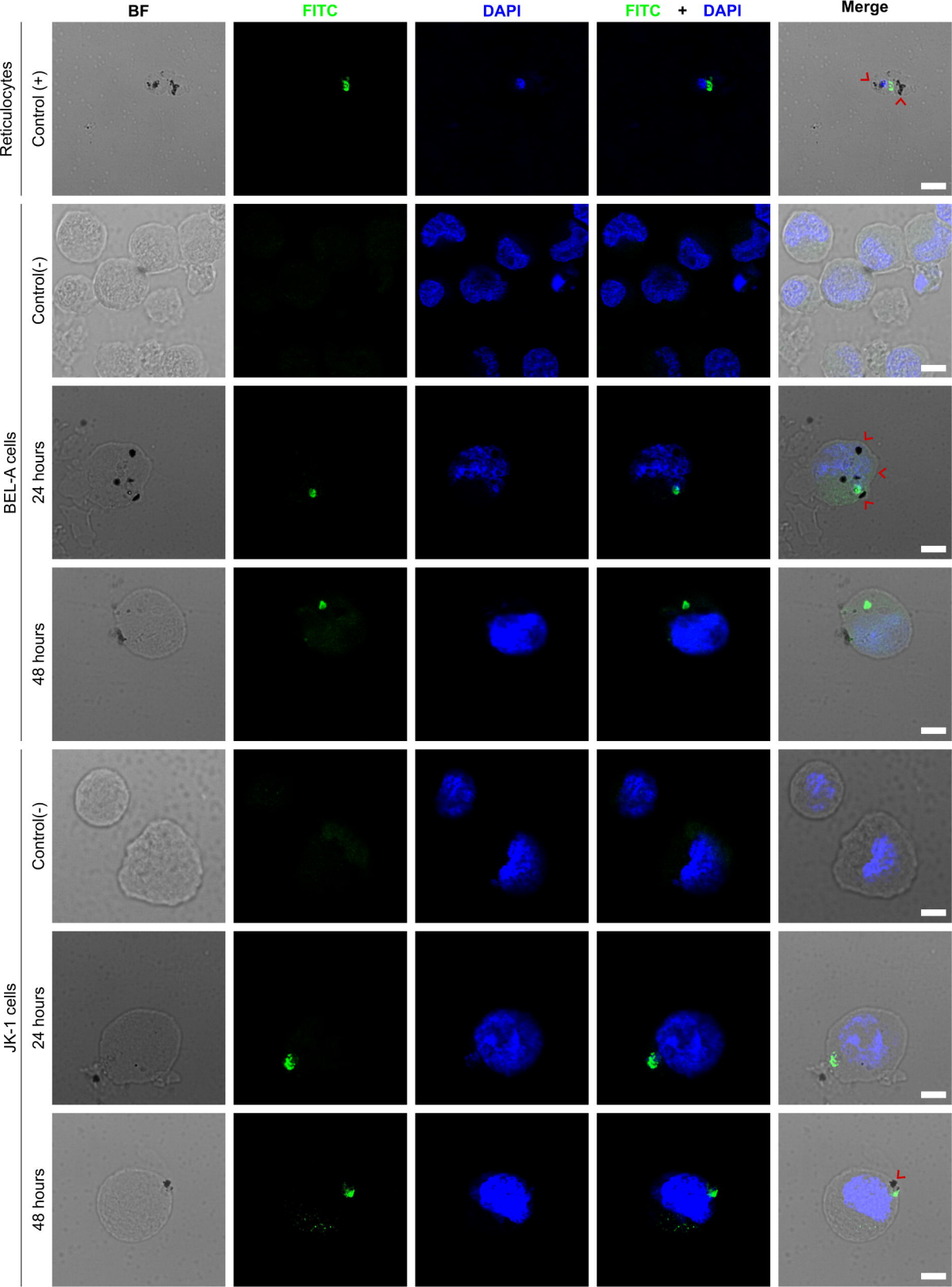
BF
FITC
DAPI
FITC + DAPI
Merge
Reticulocytes
Control (+)
BEL-A cells
Control(-)
24 hours
48 hours
JK-1 cells
Control(-)
24 hours
48 hours

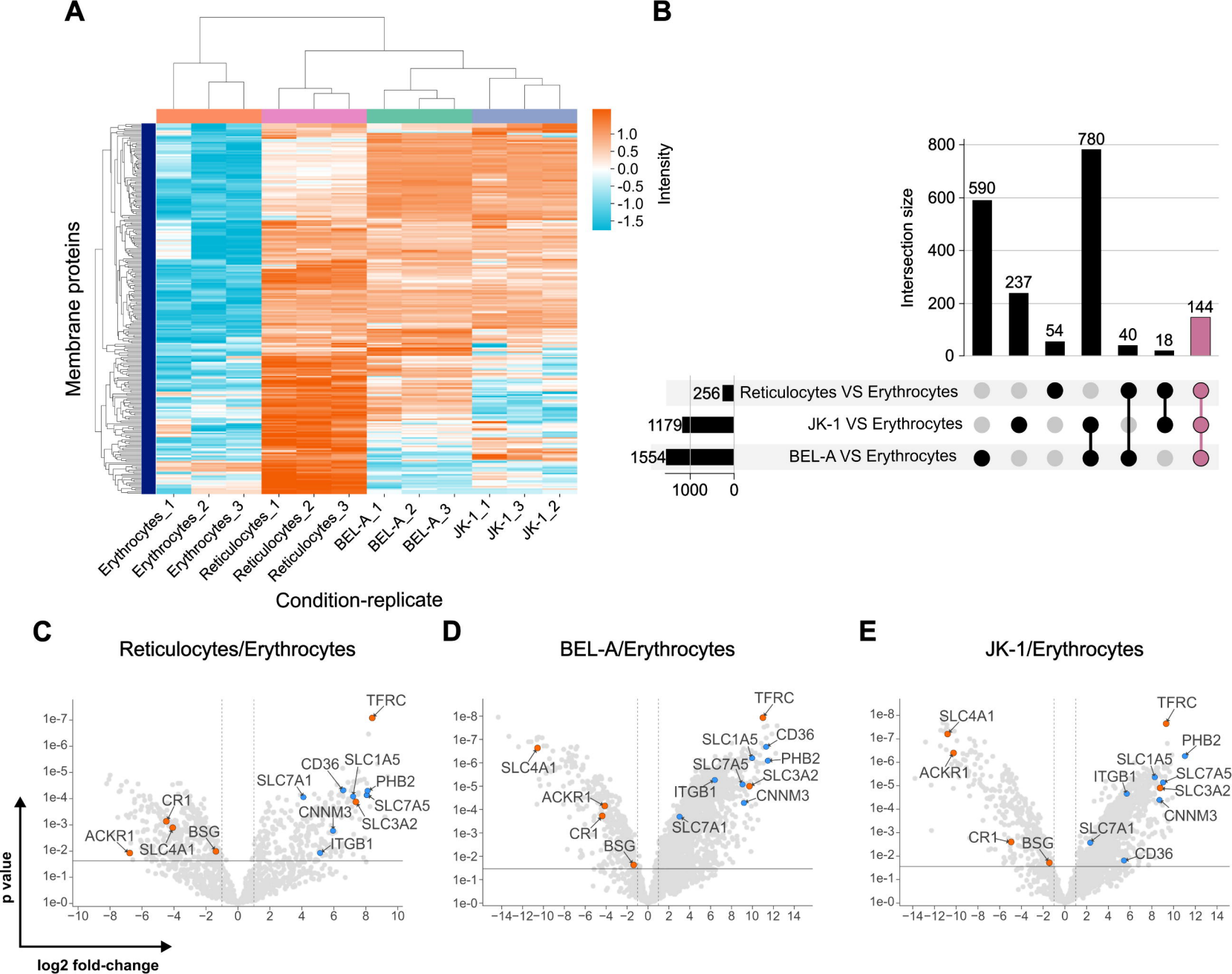
A
Membrane proteins
Intensity
1.0
0.5
0.0
-0.5
-1.0
-1.5
Erythrocytes_1
Erythrocytes_2
Erythrocytes_3
Reticulocytes_1
Reticulocytes_2
Reticulocytes_3
BEL-A_1
BEL-A_2
BEL-A_3
JK-1_1
JK-1_3
JK-1_2
Condition-replicate
B
Intersection size
800
600
400
200
0
590
237
54
780
40
18
144
256
1179
1554
1000
0
Reticulocytes VS Erythrocytes
JK-1 VS Erythrocytes
BEL-A VS Erythrocytes
C
Reticulocytes/Erythrocytes
TFRC
CD36
SLC1A5
SLC7A1
PHB2
CR1
CNNM3
SLC7A5
SLC3A2
ACKR1
BSG
SLC4A1
ITGB1
p value
log2 fold-change
D
BEL-A/Erythrocytes
TFRC
SLC1A5
CD36
SLC4A1
SLC7A5
PHB2
SLC3A2
ITGB1
ACKR1
CNNM3
CR1
SLC7A1
BSG
E
JK-1/Erythrocytes
TFRC
SLC4A1
PHB2
SLC1A5
ACKR1
ITGB1
SLC7A5
SLC3A2
CNNM3
SLC7A1
CR1
BSG
CD36

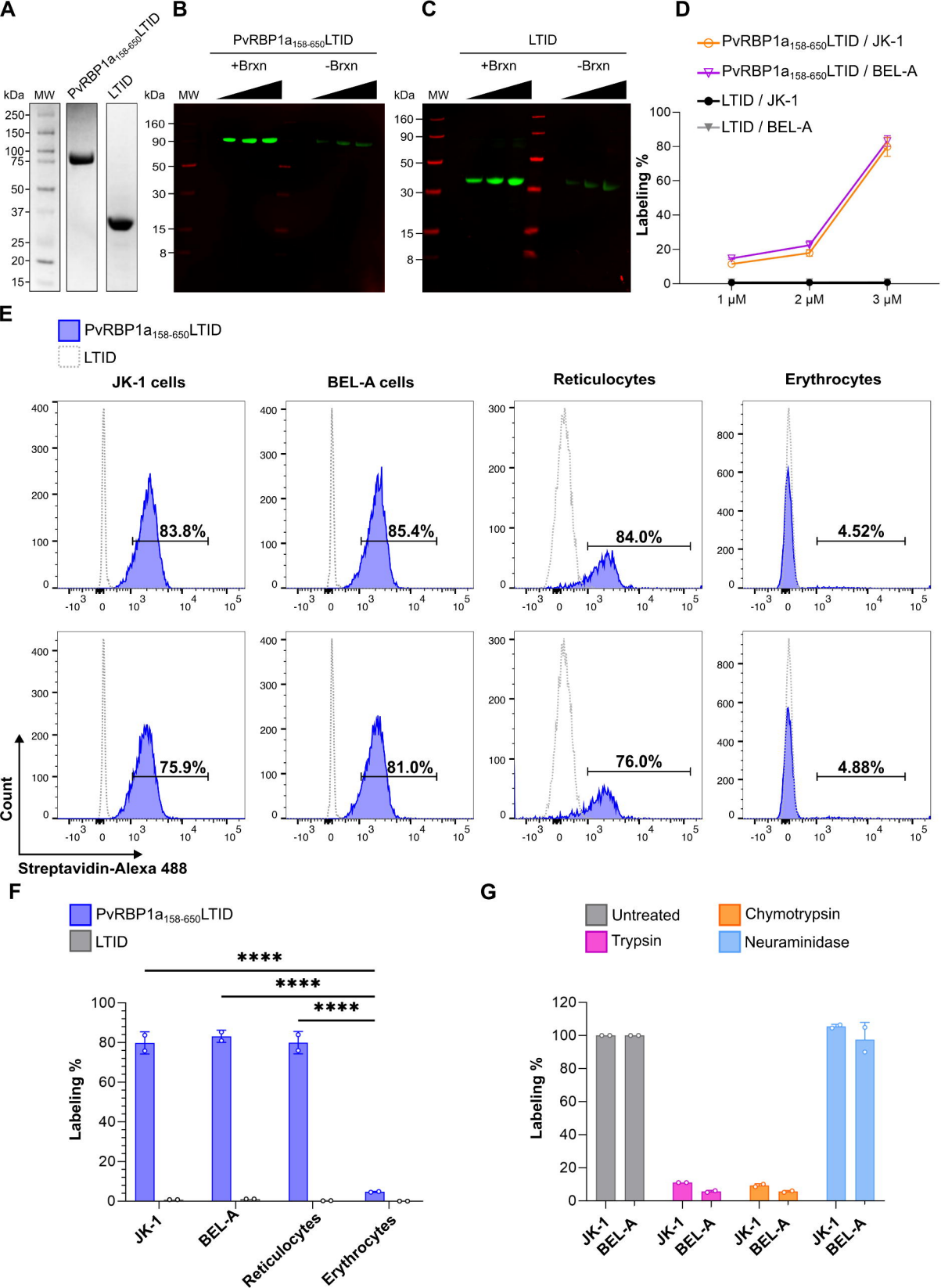
A
kDa
MW
PvRBP1a158-650LTID
LTID
250
150
100
75
50
37
25
20
15
B
PvRBP1a158-650LTID
+Brxn
-Brxn
kDa
MW
160
90
50
30
15
8
C
LTID
+Brxn
-Brxn
kDa
MW
160
90
50
30
15
8
D
PvRBP1a158-650LTID / JK-1
PvRBP1a158-650LTID / BEL-A
LTID / JK-1
LTID / BEL-A
Labeling %
100
80
60
40
20
0
1 μM
2 μM
3 μM
E
PvRBP1a158-650LTID
LTID
JK-1 cells
BEL-A cells
Reticulocytes
Erythrocytes
83.8%
85.4%
84.0%
4.52%
75.9%
81.0%
76.0%
4.88%
Count
Streptavidin-Alexa 488
F
PvRBP1a158-650LTID
LTID
****
****
****
Labeling %
JK-1
BEL-A
Reticulocytes
Erythrocytes
G
Untreated
Chymotrypsin
Trypsin
Neuraminidase
Labeling %
JK-1
BEL-A

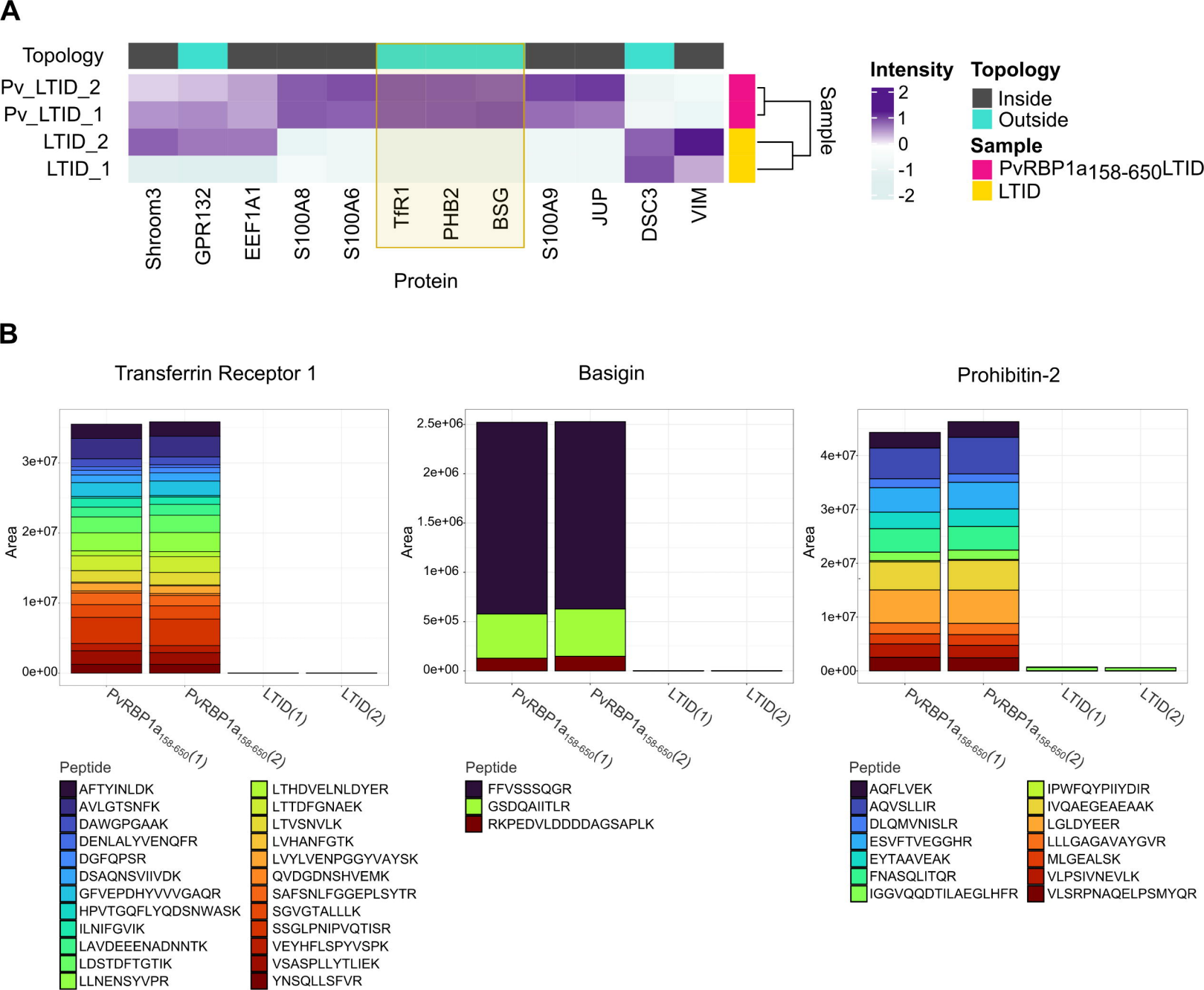
A
Topology
Pv_LTID_2
Pv_LTID_1
LTID_2
LTID_1
Shroom3
GPR132
EEF1A1
S100A8
S100A6
TfR1
PHB2
BSG
S100A9
JUP
DSC3
VIM
Protein
Sample
Intensity
2
1
0
-1
-2
Topology
Inside
Outside
Sample
PvRBP1a158-650LTID
LTID
B
Transferrin Receptor 1
Basigin
Prohibitin-2
Area
PvRBP1a158-650(1)
PvRBP1a158-650(2)
LTID(1)
LTID(2)
Peptide
AFTYINLDK
AVLGTSNFK
DAWGPGAAK
DENLALYVENQFR
DGFQPSR
DSAQNSVIIVDK
GFVEPDHYVVVGAQR
HPVTGQFLYQDSNWASK
ILNIFGVIK
LAVDEEENADNNTK
LDSTDFTGTIK
LLNENSYVPR
LTHDVELNLDYER
LTTDFGNAEK
LTVSNVLK
LVHANFGTK
LVYLVENPGGYVAYSK
QVDGDNSHVEMK
SAFSNLFGGEPLSYTR
SGVGTALLLK
SSGLPNIPVQTISR
VEYHFLSPYVSPK
VSASPLLYTLIEK
YNSQLLSFVR
FFVSSSQGR
GSDQAIITLR
RKPEDVLDDDDAGSAPLK
AQFLVEK
AQVSLLIR
DLQMVNISLR
ESVFTVEGGHR
EYTAAVEAK
FNASQLITQR
IGGVQQDTILAEGLHFR
IPWFQYPIIYDIR
IVQAEGEAEAAK
LGLDYEER
LLLGAGAVAYGVR
MLGEALSK
VLPSIVNEVLK
VLSRPNAQELPSMYQR

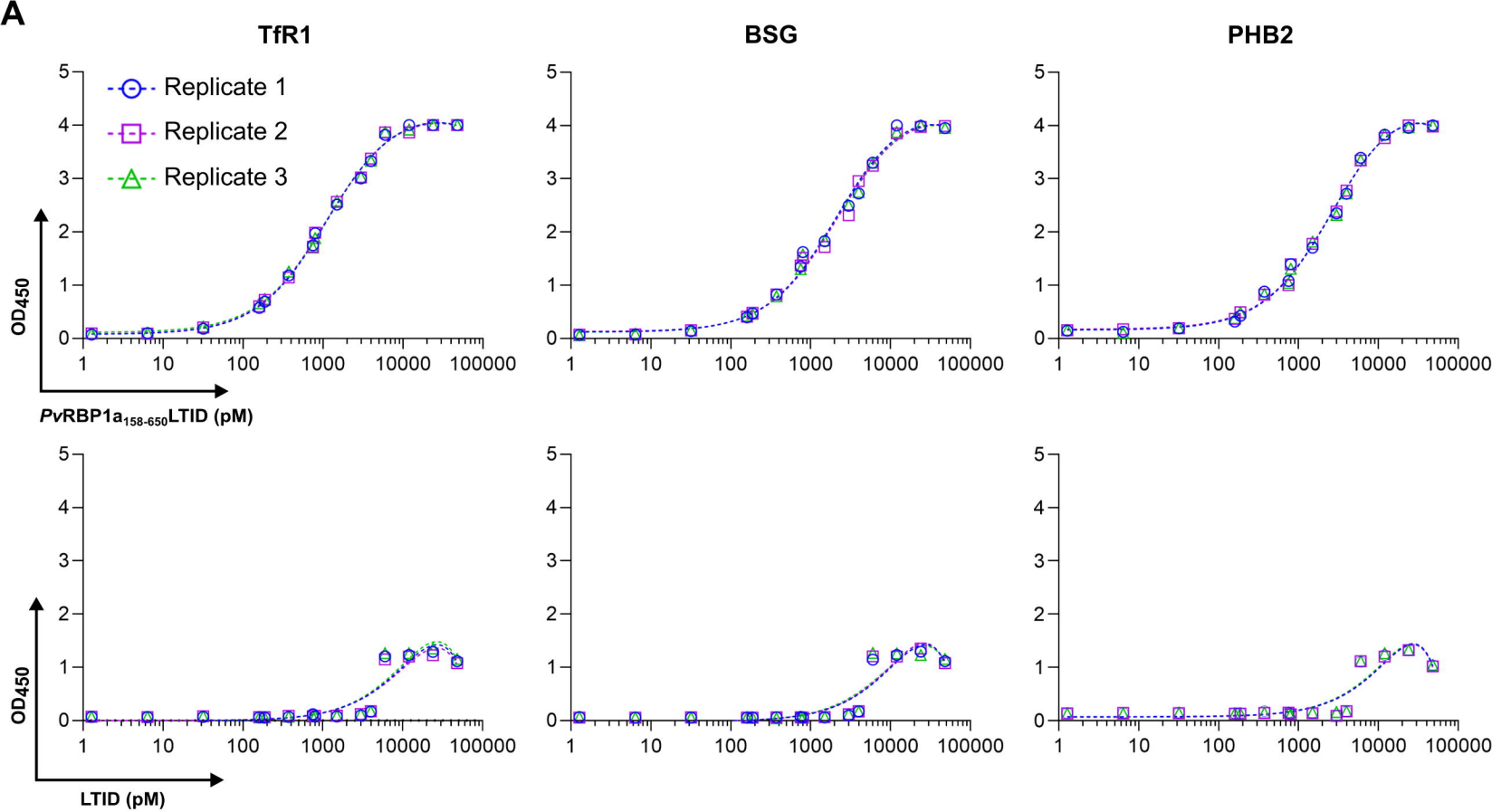
A
TfR1
BSG
PHB2
Replicate 1
Replicate 2
Replicate 3
OD450
PvRBP1a158-650LTID (pM)
LTID (pM)
0
1
2
3
4
5
1
10
100
1000
10000
100000

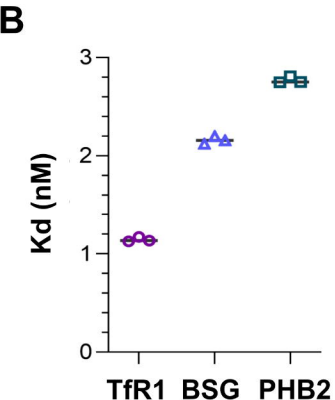
B
Kd (nM)
0
1
2
3
TfR1
BSG
PHB2